

# INTERPRETATION OF THE NON-THERMAL BREMSSTRAHLUNG EMISSION DURING LH CURRENT DRIVE ON TORE SUPRA

Y. Peysson, F. Imbeaux and E. Joffrin

Association EURATOM-CEA sur la Fusion Contrôlée  
CEA Cadarache - 13108 Saint-Paul-lez-Durance Cedex, France

**Abstract.** Using the new hard x-ray tomographic system installed on TORE SUPRA, a benchmark of ray-tracing and wave diffusion codes describing the Lower Hybrid dynamics in tokamak plasmas is carried out.

## 1. Introduction

The recent availability of a high spatial resolution tomographic system in the hard x-ray (HXR) energy range on TORE SUPRA has allowed to investigate the problem of the Lower Hybrid (LH) power deposition profile during non-inductive current drive experiments, at a level of accuracy which has never been obtained so far on a large tokamak [1]. The non-thermal bremsstrahlung emission offers indeed a quite direct insight on the build-up of the fast electron distribution function, both in velocity and configuration spaces. In this paper, comparisons between experimental observations and numerical calculations are presented in view to benchmark code capabilities for prediction of the radial dependence of LH power absorption, a critical assessment for an effective control of the current density profile in tokamak plasmas.

Experiments are restricted to moderate input power level ( $P_{LH} \leq 2$  MW) so that modifications of the plasma equilibrium by the LH-driven current may be considered as negligible, an assumption which is usually considered in models describing the LH wave dynamics. When such a condition is fulfilled, reliable benchmarks of numerical codes against experiments may be carried out. Calculations are based on two models, *WDFP-1D* [2], which describes the wave dynamics as a diffusion process in the phase space (very weak absorption limit), and *RT/FP-2D*, where the LH energy flow in the plasma is determined by a standart ray-tracing technique in toroidal geometry [3]. For *WDFP-1D*, the wave absorption in velocity space is estimated by a 1D Fokker-Planck equation, while for *RT/FP-2D*, a full 2D relativistic Fokker-Planck solver is used [4]. The influence of the toroidal magnetic ripple, which reaches 7% at the plasma edge on TORE SUPRA, on the ray dynamics is also investigated with the help of the *RT/FP-2D* code [5]. For all ray-tracing calculations a large number of rays at launch is used (400), since the stochastic nature of the ray dynamics comes fully into play for the prediction of the LH power absorption.

## 2. Experimental set-up

The fast electron tomographic system is designed to record the non-thermal bremsstrahlung emission in the x-ray energy range between 20 and 200 keV, with requirements of high time - down to 4 ms - and space resolutions - 5 cm in the equatorial mid-plane. Horizontal and vertical cameras are made of 21 and 38 CdTe detectors respectively, as shown in Fig. 1. For each chord, a coarse spectrometry is carried out by 8 energy channels of width 20 keV. All recorded signals are first filtered by a singular value decomposition (SVD) technique to identify and remove the noise level. Local emission profiles are then obtained using a Fischer's inversion procedure. During these low power LH experiments, the thermal contribution to the bremsstrahlung emission is always negligible in the range of energy investigated by the tomographic system, as well as the noise induced by neutrons which results from thermonuclear D-D reactions of residual deuterium in helium plasmas. Data consistency between the vertical

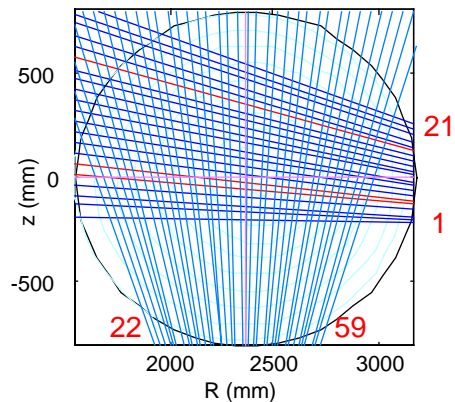


Fig. 1. HXR Tomographic system

and horizontal cameras, which is crucial to perform Abel inversion, gives a high level of confidence in the determination of the local HXR emission profiles.

### 3. HXR experimental results and numerical simulations

Since the LH wave accessibility scales as  $\sqrt{n_e}/B_t$ , parametric dependences vs. the toroidal magnetic field  $B_t$  and the electron density  $n_e$  have been performed at fixed input power level ( $P_{LH} = 0.8$  MW,  $n_{/0} = 1.8$ ), plasma current ( $I_p = 0.8$  MA), plasma size ( $a_p = 0.75$  m, circular shape) and position ( $R_p = 2.33$  m). The impurity level remains nearly constant from shot to shot, and the measured effective charge  $Z_{eff}$  is less than 4 in most cases (He plasmas).

For a central electron density of the order of  $n_{e0} \approx 2.0 \times 10^{19} \text{ m}^{-3}$ , the decrease of the toroidal magnetic field from  $B_t = 3.9$  to  $2.0$  T leads to a broadening of the HXR emission profile, which becomes slightly hollow as shown in Fig.2a. Conversely, when the electron density rises at fixed  $B_t = 3.9$  T, the radial width of the HXR emission is progressively smaller and a narrow peak at the radial position  $\rho = r/a_p \approx 0.15$  can be well identified, especially for the highest density case (Fig. 2b). Within the radial accuracy of the diagnostic, no relevant sharp structures are observed in the HXR emission profiles.

Using *WD/FP-1D*, radial widths of all predicted HXR emission profiles are systematically much smaller than experimental observations (Fig. 3a -b). This difference, which is far beyond experimental uncertainty, may not be ascribed to a large radial diffusivity of the fast electrons accelerated by the LH wave. Both transient evolutions and stationary hollow HXR emission profiles are in agreement with a low diffusion rate of the order of  $0.1 \text{ m}^2 \cdot \text{s}^{-1}$ , as deduced from previous analysis [6]. Parametric variations of the predicted LH power deposition by the code *WD/FP-1D* are critically dependent of the radial profile of the safety factor  $q(\rho)$ , which sets the internal wave boundary propagation domain and the electron temperature profile  $T_e(\rho)$  for the location of the dominant wave absorption. Since  $T_e$  remains very low in all studied experiments ( $1.9 \text{ keV} \leq T_{e0} \leq 3.7 \text{ keV}$ ), radial evolutions of the LH power deposition are mainly governed by  $q_0 = q(\rho = 0)$ , when  $q(\rho)$  is monotonic. Hence, the small outward radial shift of the LH power absorption which is predicted when  $B_t$  decreases is mainly a consequence of the variation of  $q_0$  from 0.75 to 0.84 as observed experimentally and confirmed by equilibrium simulations (Fig. 4a). Even if a similar radial shift of the HXR profile is also observed experimentally (Fig. 3a), its amplitude is much more important than predicted by the *WDFP-1D* code and may not be reproduced by changing values of  $q(\rho)$  and  $T_e(\rho)$  in the calculations, within the estimated interval of uncertainty. Predictions of the density scan at fixed  $B_t$ , exhibit also large discrepancies with the experimental observations, in particular at the highest density value (Fig. 3b), which cannot be understood by any variations of the plasma parameters within a reasonable interval. The large deviation observed at high density results mainly from the large value of  $q_0$  for the highest density discharge, which is of the order of 1.3.

Large differences between experimental results and numerical predictions are also observed with the *RTFP-2D* code, though some interesting features of the HXR signal may be qualitatively reproduced, as the broad nature of the LH power deposition profile. By lowering  $B_t$ , the fraction of LH power deposited in the core of the plasma is reduced, as shown in Fig.4a and 5a, in qualitative agreement with experimental observations (Fig. 2a). However, the two-peak structure predicted by *RTFP-2D* is never observed experimentally. Ray-tracing simulations in an axisymmetric topology are not able to reproduce the density scan (Fig. 4b). Conversely, the HXR profiles at the two highest density cases may be well described by the *RTFP-2D* code, providing magnetic ripple corrections are taken into account in the LH wave dynamics (Fig. 5b).

The effect of the plasma current has been also investigated, at fixed  $B_t = 3.9$  T and  $n_{e0} \approx 2.0 \times 10^{19} \text{ m}^{-3}$ . As shown in Fig. 2c, the increase of  $I_p$  from 0.8 MA to 1.2 MA leads to a large broadening of the plasma, already reported in previous experiments [5]. Such a change cannot be reproduced by the *WDFP-1D* code (Fig. 3c), as well the *RTFP-2D* one, when magnetic ripple corrections are neglected (Fig. 4c). However, a slight broadening of the LH power deposition profile is predicted, if the magnetic ripple perturbation is included in the ray dynamics (Fig. 5c).

## 4. Conclusion

Reliable experimental HXR profiles have been obtained using the new hard x-ray tomographic system on TORE SUPRA. From the available database, systematic benchmarks of three different models which describe the LH wave dynamics in the plasma have been carried out: toroidal magnetic scan, electron density scan and plasma current scan. It turns out that large discrepancies are observed between experimental results and numerical results, though some tendencies may be qualitatively reproduced, especially using the ray-tracing code with toroidal magnetic ripple corrections. These substantial differences suggest that additional ingredient should be added to describe accurately the LH wave propagation and absorption in the weak

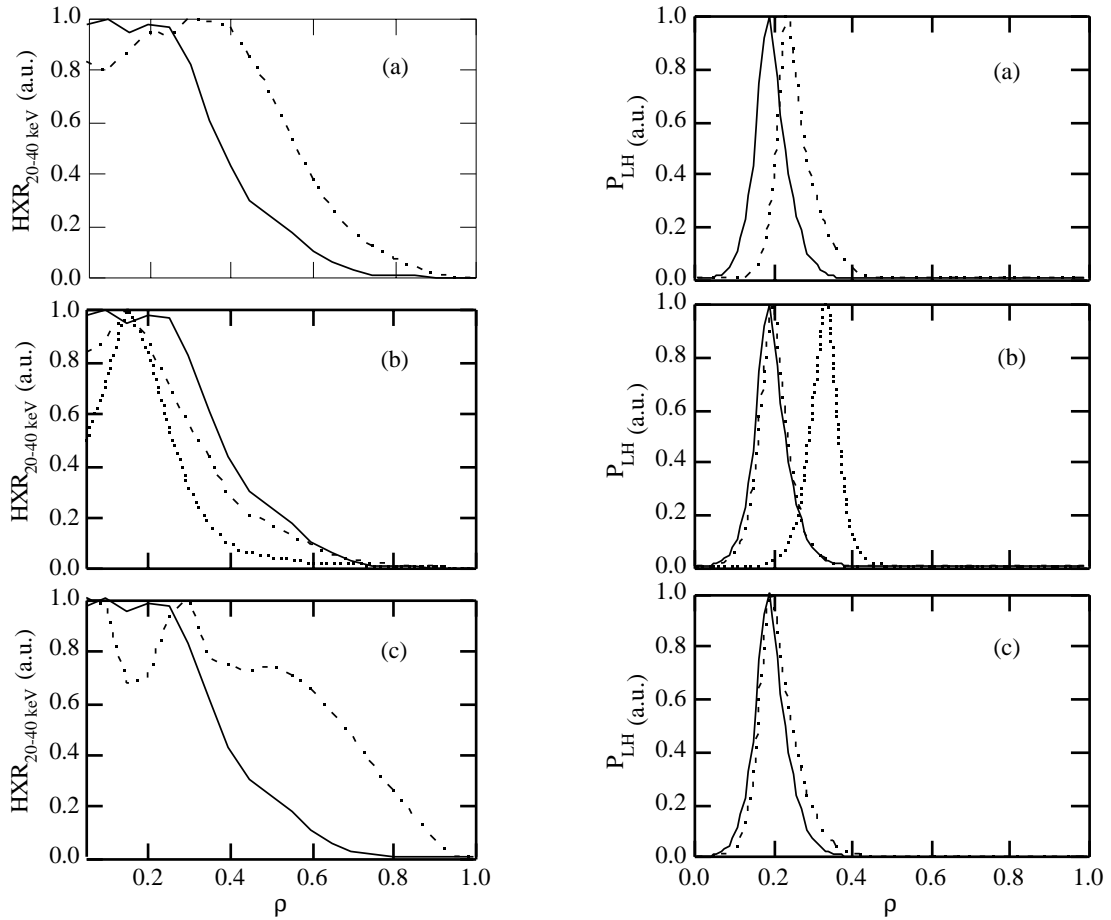


Fig.2. Experimental HXR radial profiles. (a) Magnetic field scan,  $I_p = 0.8$  MA,  $n_{e0} \approx 2.0 \times 10^{19} \text{ m}^{-3}$ , solid line: corresponding to a very weak damping limit [4]. (a)  $B_t = 3.9$  T, dot-dashed line:  $B_t = 2.0$  T. (b) Density scan,  $I_p = 0.8$  MA,  $B_t = 3.9$  T, solid line:  $n_{e0} = 2.1 \times 10^{19} \text{ m}^{-3}$ , dot-dashed line:  $n_{e0} = 3.9 \times 10^{19} \text{ m}^{-3}$ , those in Fig. 2. dashed line:  $n_{e0} = 5.6 \times 10^{19} \text{ m}^{-3}$ . (c) Plasma current scan,  $B_t = 3.9$  T,  $n_{e0} \approx 2.0 \times 10^{19} \text{ m}^{-3}$  solid line:  $I_p = 0.8$  MA, dot-dashed line:  $I_p = 1.2$  MA.

Fig. 3. Simulations using the WDFP-1D code, Magnetic field scan. (b) Electron density scan. (c) Plasma current scan. Lines in Fig. 3 are similar to those in Fig. 2.

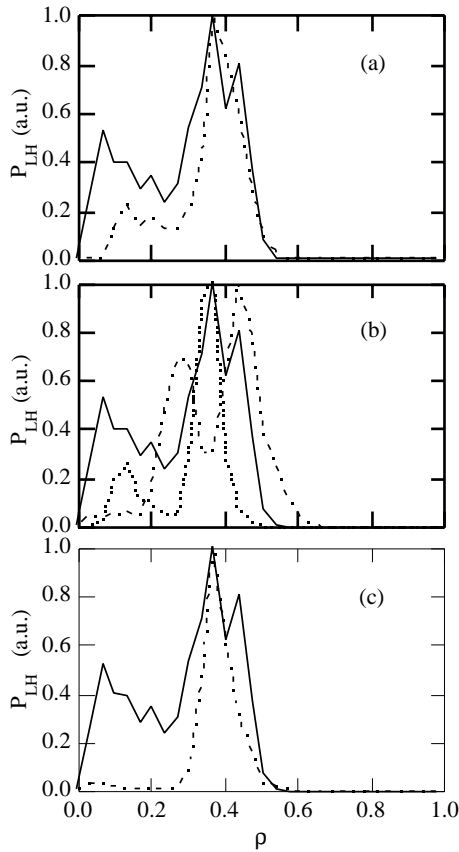


Fig. 4. Simulations using the RTFP-2D code, in an axisymmetric topology [5]. (a) Magnetic field scan. (b) Electron density scan. (c) Plasma current scan. Lines in Fig. 4 are similar to those in Fig. 2.

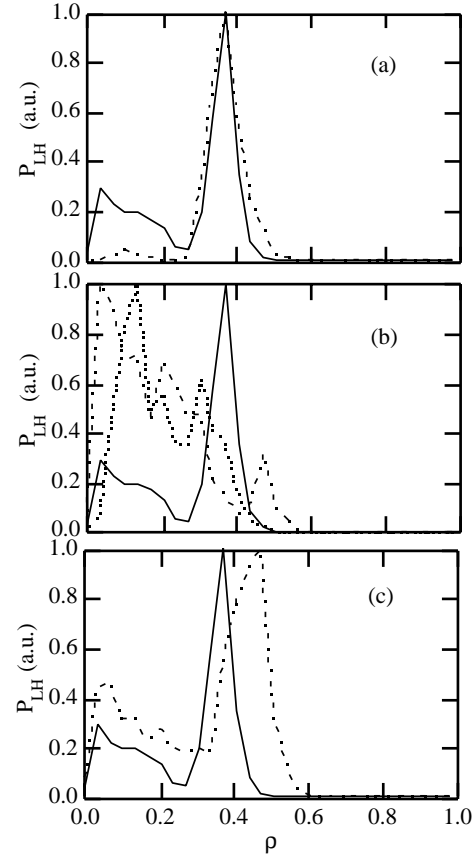


Fig. 5. Simulations using the RTFP-2D code, including toroidal magnetic field corrections [5]. (a) Magnetic field scan. (b) Electron density scan. (c) Plasma current scan. Lines in Fig. 5 are similar to those in Fig. 2.

damping regime, like density or magnetic fluctuations in the plasma. Such an analysis clearly demonstrates that most important available codes are not able to explain the experimental phenomenology when the stochastic nature of the ray dynamics is important, and therefore their use to predict the LH power deposition for transport analysis in these conditions is highly questionable. The experimental fact that HXR profiles remain roughly centered and rather broad, whatever plasma conditions is the clear signature that LH power absorption is nearly independent of the initial parameters of the wave at launch. This weak damping regime which prevents any robust control of the LH power deposition of the wave, may be avoided in low temperature plasmas by an appropriate choice of the launching poloidal angle, as shown on recently on JT60-U [7].

### Acknowledgements

The help of T. Hoang and T. Aniel for data analysis is greatly acknowledged.

### References

- [1] Y. Peysson et al., 24th EPS Conf. Contr. Fus. Plasma Phys., Berchtesgaden, Germany, 21A, 229 (1997)
- [2] K. Kupfer et al., Phys. Fluids, **5**, 4391 (1993).
- [3] P. Bonoli and R.C. Englade, Phys. Fluids, **29**, 2937 (1986).
- [4] Y. Peysson et al., 11th Top. Conf. RF power in Plasmas, Palm Spring, USA, **355**, 102 (1995).
- [5] Y. Peysson et al., Phys. Plasmas, **3**, 3668 (1996).
- [6] Y. Peysson, Plasma Phys. Controlled Fusion, **35**, B253 (1993).
- [7] H. Kimura et al., 11th Top. Conf. RF power in Plasmas, Palm Spring, USA, **355**, 81 (1995).